Journal of
Ship&Ocean
Technology
©DECEMBER 2003

SOTECH Vol. 7, No. 4, pp. 41~49, 2003

Prediction of Welding Deformation of Ship Hull Blocks

C. D. Jang[1] and C. H. Lee[2]

[1]Department of Naval Architecture & Ocean Engineering, Seoul National University, RIMSE, Seoul, Korea; E-mail: cdjang@snu.ac.kr
[2]Samsung Heavy Industries CO., LTD.

Abstract

Welding deformation reduces the accuracy of ship hull blocks and decreases productivity due to the need for correction work. Preparing an error-minimizing guide at the design stage will lead to higher quality as well as higher productivity. Therefore, developing a precise method to predict the weld deformation is an essential part of it. This paper proposes an efficient method for predicting the weld deformation of complicated structures based on the inherent strain theory combined with the finite element method. A simulation of a stiffened panel confirmed the applicability of this method to simple ship hull blocks.

Keywords: welding deformation, accuracy management, ship hull blocks, inherent strain, highest temperature, degree of restraint, assembly sequence, finite element method

1 Introduction

Accuracy management in shipbuilding is an essential technique to systematize the work process of fabrication, assembly, pre-erection and erection. In particular, the work efficiency in the erection stage is dependent on the accuracy of the blocks.

However, welding deformation accumulated in each assembly stage reduces the accuracy of the blocks and has an adverse effect on productivity. Therefore, an analysis method to estimate welding deformation is essential for proposing error-minimizing guides at the design stage.
The requirements for the analysis method are as follows,

1) It should be accurate.

2) The shape change of a block according to assembly processes should be considered.

3) It should be efficient in time and cost.

In this paper, a method for predicting the welding deformation of large structures is presented. The method uses both the inherent strain theory and the experimental results combined with the finite element method for accurate and efficient analysis. In the inherent strain theory, the residual plastic strain due to welding is defined as the inherent strain. Assuming the inherent strain is the initial strain, welding deformation can be easily calculated by elastic FE analysis, omitting the complicated thermal elastic-plastic FE analysis. Jang et al(1996) estimated the inherent strain region and

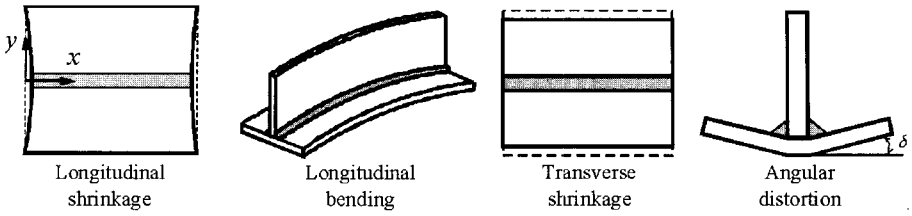

Figure 1: Types of welding deformation

represented the inherent strain as a function of the mechanical melting temperature (Ueda 1995) and the degree of restraint Murakawa et al(1997) used a simplified analysis model to obtain the inherent strain. They represented the inherent strain as a function of the highest temperature and degree of restraint. However, this method has limitations in applying to complicated structures. Seo and Jang(1999) calculated the deformation of large structure using the unit loading method to obtain the degree of restraint. In this paper, the welding deformation of a stiffened plate as a part of hull block was calculated using equivalent load method based on inherent strain analysis. In addition, the efficiency and effectiveness of the proposed method was verified by comparing with the experimental results.

2 Inherent strain due to welding

In the welding process, the heat input around a weld joint causes a non-uniform temperature distribution and thermal stress. As a result, the plastic strain remains around the weld bead and permanent deformation occurs after welding. The plastic strain that causes the welding deformation can be defined as the inherent strain. In general, the inherent strain caused by welding has six components according to their directions. However, in the case where a plate has a large length/thickness ratio such as a ship hull plate, only two components ε_x^* and ε_y^* are dominant. Some typical types of welding deformation due to inherent strain are shown in Figure 1.

2.1 Calculation of the inherent strain

The inherent strain distribution can be formulated using a simplified thermal elastic-plastic analysis model as shown in Figure 2 (Jang 1996). The welding region, where the inherent strain occurs, can be modeled as a bar and a spring.

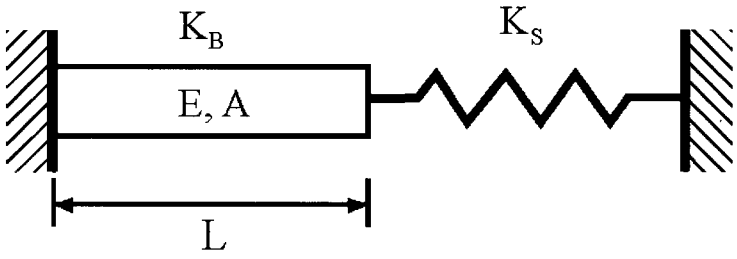

Figure 2: Simplified elastic-plastic analysis model

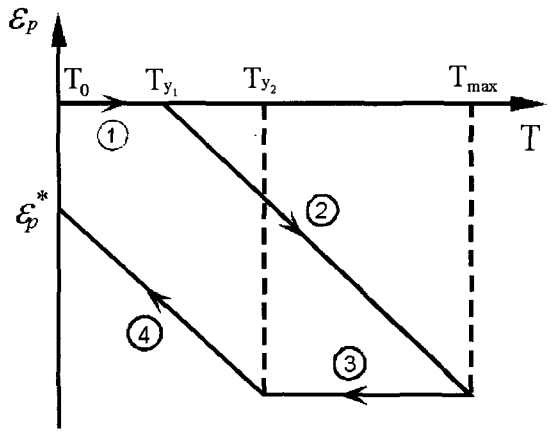

Figure 3: Thermal history of plastic strain

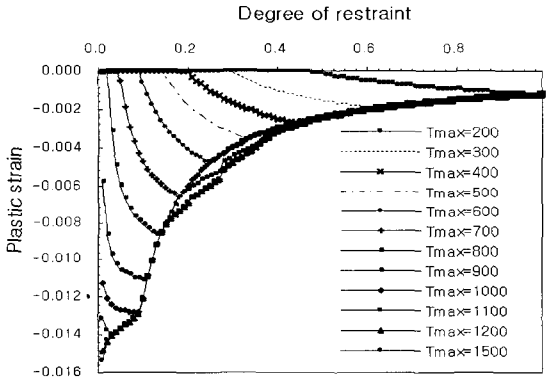

Figure 4: Residual plastic strain

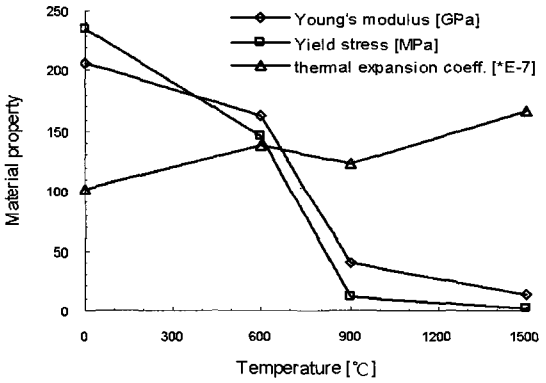

Figure 5: Temperature dependent material properties

The thermal history of the inherent strain according to the temperature change of a bar can be divided into four steps, as shown in Figure 3. After all the thermal history the compressive plastic strain remains as an amount of ε_p^*. The magnitude of residual plastic strain was calculated from the total strain, the stress-strain relation and the equilibrium equation of a bar-spring system.

Total strain:

$$\varepsilon = \varepsilon_{th} + \varepsilon_e + \varepsilon_p \tag{1}$$

Stress-strain relation:

$$\sigma = E\varepsilon_e \tag{2}$$

Equilibrium equation:

$$F_B = F_S \tag{3}$$

Figure 4 shows the calculation results of the residual plastic strain. The material of the bar is

mild steel and temperature dependency is considered as shown in Figure 5.

2.2 Distribution of the highest temperature

Heat transfer analysis was conducted to calculate the temperature distribution of welded structures. The welding heat source was modeled as a normal distributed moving heat flux. And the highest temperature was calculated.

2.3 Calculation of degree of restraint

The degree of restraint represents the level of resistance against the thermal deformation of the welding region. The degree of restraint of stiffened panel was determined from the analogy of the bar-spring model in the case of the simplified analysis model.

3 Equivalent nodal loads

The equivalent forces and moments were obtained by using the inherent strain. Using the obtained equivalent nodal loads, the welding deformation could be calculated by elastic FE analysis. All types of equivalent loads are shown in Figure 6. The shrinkage force f_i can be solved using (4).

$$f_i = \frac{AE}{l} \sum_{j=1}^{N_i} \varepsilon_j^* l_j \tag{4}$$

The equivalent transverse forces and moments are calculated using (5) and (6), respectively.

$$f_y = \sum_{i=1}^{N} f_i \tag{5}$$

$$m_y = \sum_{i=1}^{N} f_i z_i \tag{6}$$

Also the longitudinal shrinkage force f_x and bending moment m_x can be calculated using inherent strain.

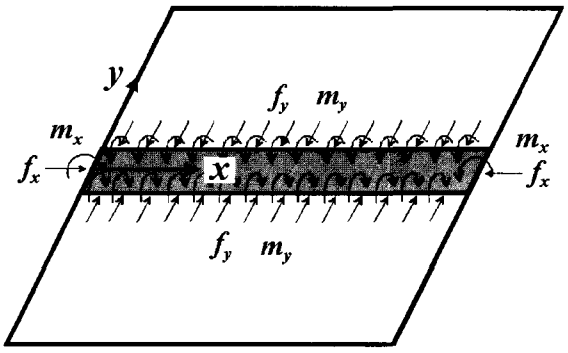

Figure 6: Equivalent loads of inherent strain

4 Simulation of welding deformation

The welding deformation of stiffened plates was simulated using both the inherent strain method and FE analysis. The simulation procedures can be summarized into three steps. The first step analyzes heat transfer to calculate temperature distribution of each welding section with the given information on welding parameters. The FE model uses heat conduction elements and considers convection on the surface. The second step computes the degree of restraint by the FE analysis. The third step calculates the inherent strain components and their equivalent loads, and the welding deformation of a structure was solved by FE analysis.

5 Calculation results

5.1 Welding deformation of simple specimen

The calculated results were compared with the experimental results in the case of a bead-on-plate and fillet welding to verify the accuracy of the proposed method. Terasaki's GMAW(gas metal arc welding) experimental results(Satoh 1976) were used for the comparison. Terasaki's experimental results were regressed with the parameter, Q/t^2, and plotted as a solid line in Figure 7. And the results of present calculations are plotted in symbolic marks. The $L \times B$ of the plate is $400 \times 400mm$ and the thickness is ranged from $8mm$ to $14mm$. And the parameter, Q/t^2, is ranged from 1000 to $5300cal/cm^3$. The parameter Q represents the heat input per unit length and t is the plate thickness. The comparison of experiment and calculation results is plotted in Figure 7.

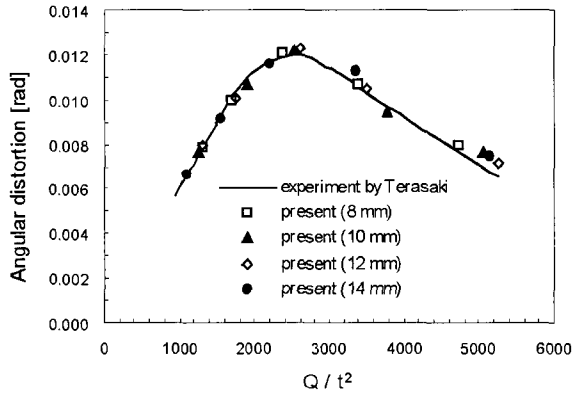

Figure 7: Comparison of angular distortion in case of bead-on-plate welding

In the case of fillet welding, the calculated results were compared with the experimental results reported by Lee et al. for CO_2 welding(Kim 1997). In Figure 8, the solid line is a regression curve of the experimental results reported by Lee et al. and the symbolic marks are the present calculation results. From the comparisons, the calculated welding deformation shows good agreement with the experimental results over the wide range of welding conditions.

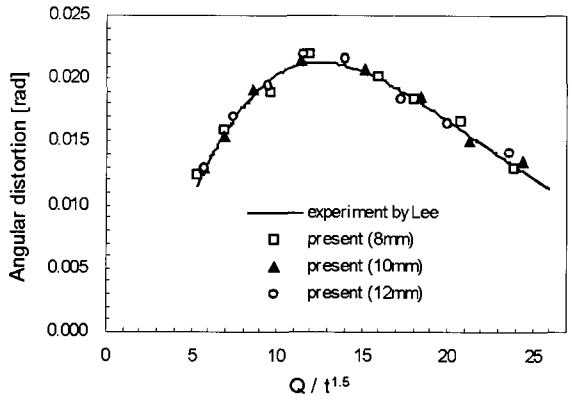

Figure 8: Comparison of angular distortion in case of fillet welding

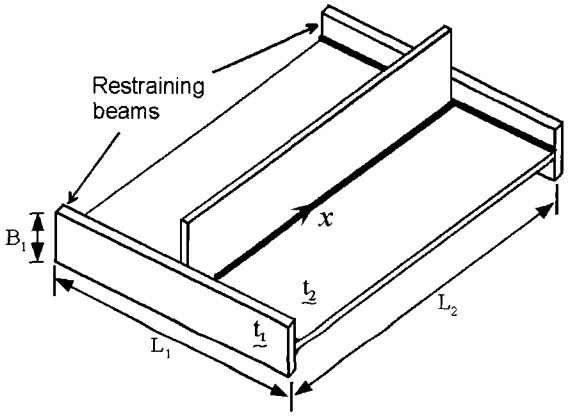

Figure 9: Fillet welding restrained by edge plates

5.2 Fillet welding with external restraints

As shown in Figure 9, restraining beams are attached at both ends of a plate. Therefore, when a stiffener is welded to this plate, the angular distortion reduces in proportion to the degree of restraint.

The angular distortion of three cases was calculated and compared with the experimental results.

(case 1) No variation of E and β
(case 2) Variation of β only
(case 3) Variation of E and β

Figure 10 shows the angular distortion ratio δ_r/δ_f for each case according to the restraining factor. δ_f is the angular distortion of the free state without restraining beams. And δ_r is the angular distortion of the restrained state, as shown in Figure 9. The calculation results are plotted in Figure 10. As the restraint factor increases, the angular distortion ratio decreases in all three cases. But case 3 chases the experimental results better than the other two cases.

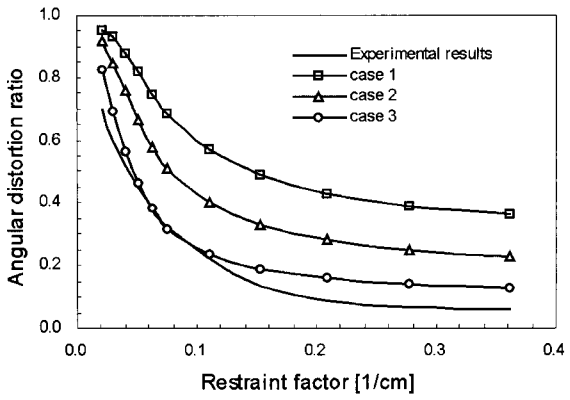

Figure 10: Comparison of angular distortion ratio

5.3 Deformation analysis of stiffened plates

It is well known that final welding deformation becomes different according to the adopted fabrication sequence. This is one of the main issues for ship building companies in determining the optimum fabrication sequence considering the operation efficiency. In this study, a stiffened plate is investigated to examine the effect of fabrication sequence. The welding deformations are calculated according to two types of fabrication sequences. The length and breadth of the base plate is $2000mm$ and $1500mm$ respectively. Figure 12 shows the results of deformation analysis according to each assembly stage of case 1. Step 4 and step 6 are the straightening stages to attach the next stiffener. The straightening stages were modeled by applying the constraining displacements. Figure 13 and Figure 14 show the vertical displacement along the x-axis and y-axis of Figure 11, respectively. The difference in the magnitude of deformation was due to the difference in the degree of restraint according to assembly sequence. As shown above, the proposed method can consider the effect of both the fabrication sequence and the practical welding conditions. Using the proposed method, a plan for reducing welding deformation can be devised.

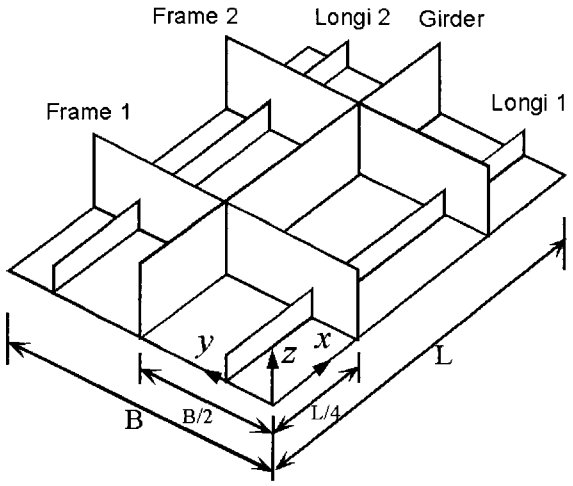

Figure 11: Shape of stiffened plate for analysis

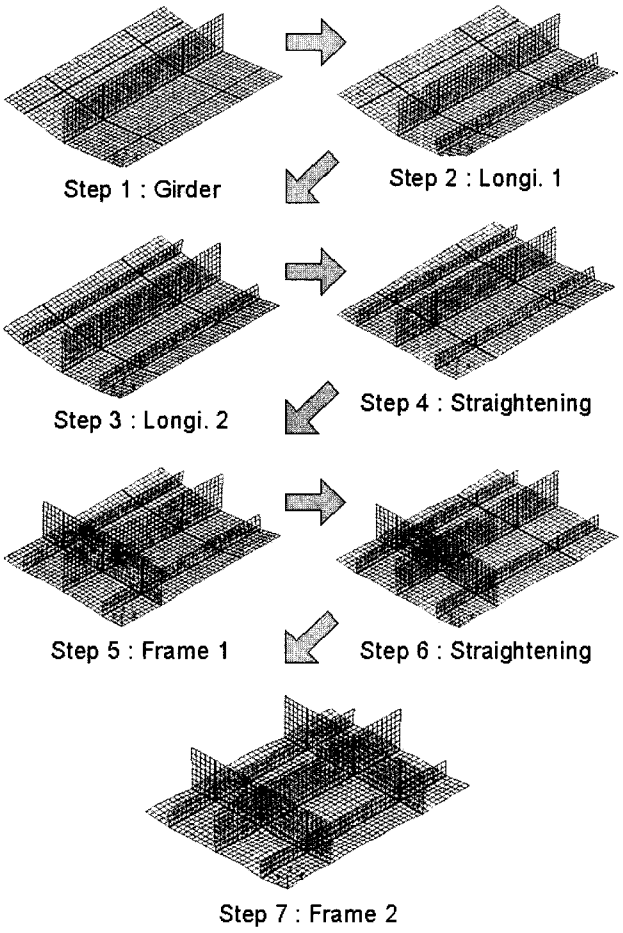

Figure 12: Welding deformation of each assembly stage (case 1)

6 Conclusions

Authors proposed a method for the estimation of welding deformation of stiffened panels as a part of ship hull blocks.
From the simplified thermal elasto-plastic analysis, the inherent strain at a point was determined by using the anlogy of the bar–spring model.
The accuracy of the proposed method was confirmed by comparing the calculated results with the experimental results in the bead-on-plate and fillet welding cases.
In particular, an attempt to obtain more accurate inherent strains by considering the effects of the temperature increase and assembly sequence was made.
Furthermore, the effect of the fabrication sequences on the welding deformation was studied by considering fabrication stage.
From the simulation of stiffened panels which are widely used in shipbuilding, it is verified that the proposed method can be utilized in prediction and control of welding distortions in ship hull blocks efficiently.

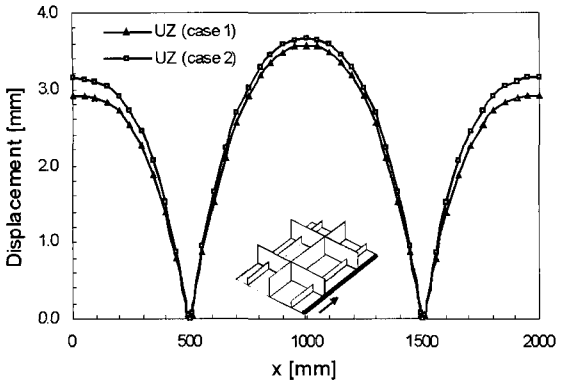

Figure 13: Vertical displacement along x-axis

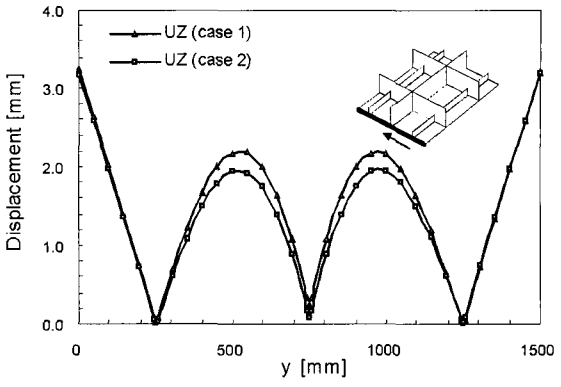

Figure 14: Vertical displacement along y-axis

References

JANG, C.D. AND SEO, S.I. 1996 A study on the automatic fabrication of welded built-up beams. Trans. of the Society of Naval Architects of Korea, **33(1)**, pp. 206-213

KIM, S.I., HAN, J.M., CHO, Y.K., KANG, J.K. AND LEE, J.Y. 1997 A study on the accuracy control of block assembly in shipbuilding. ICCAS '97, pp. 367- 381

MASUBUCHI, K. 1980 Analysis of welded structures. Pergamon Press, pp. 239-243

MURAKAWA, H., LUO, Y. AND UEDA, Y. 1997 Prediction of welding deformation and residual stress by elastic FEM based on inherent strain. J. of the society of naval architects of Japan, **180**, pp. 739-751

SATOH, K. AND TERASAKI, T. 1976 Effect of welding conditions on welding deformations in welded structural materials. J. of the Japanese welding society, **45(4)**, pp. 302-308

SEO, S.I. AND JANG, C.D. 1999 A study on the prediction of deformations of welded ship structures. Journal of Ship Production, **15(2)**, pp. 73-81

TEKRIWAL, P. 1989 Three-dimensional transient thermo-elasto-plastic modeling of gas metal arc welding using the finite element method. Ph. D. thesis, U. of Illinois at Urbana-Champaign, Urbana, Ill., U.S.A.

UEDA, Y. AND MA, N.X. 1995 Measuring Methods of Three-Dimensional Residual Stresses with Aid of Distribution Function of Inherent Strains(Report 3). Trans. of Japanese Welding Research Institute, **24(2)**, pp. 123-130

WATANABE, M. AND SATOH, K. 1965 Welding mechanics and its applications. Asakura Publication, pp. 367- 411